Raman Study of Stable and Metastable Structures of Phenylacetylene in Acetonitrile

H. Abramczyk,* B. Brożek, G. Waliszewska, and J. P. Suwalski

Technical University, Institute of Applied Radiation Chemistry, 93-590 Łódź, Wróblewskiego 15 street, Poland

Received: March 29, 2001; In Final Form: October 19, 2001

Raman spectra of the $\nu_s(\equiv C-H)$ stretching mode as well as Raman spectra in the lattice region of 15−200 cm^{-1} of phenylacetylene (PA) dissolved in acetonitrile in frozen matrixes and liquid solutions as a function of concentration, temperature, and quenching rate have been recorded in the range of 77−293 K. The optical measurements were complemented by the differential scanning calorimetry (DSC) scans. The results reveal some dramatic changes with concentration, temperature, and quenching rate and are of potential relevance both to fundamental condensed phase modeling and to liquid crystal technology. We have discussed the origin of the vibrational substructure observed for the $\nu_s(\equiv C-H)$ stretching mode of PA, and we have found that it represents stable and metastable crystal phases as well as nonequilibrium glassy crystal phases. Low temperature polymorphism in mixtures of PA in acetonitrile in the full concentration range has been characterized. We have found that the low temperature polymorphism of PA strongly depends on the concentration, temperature, and quenching rate.

1. Introduction

The formation of a crystal or a glass is a complicated process that depends on many factors such as interactions with impurities, interfaces, sample volume, and quenching rate. Phase transition between liquid and solid represents a variety of physical processes. Some systems undergo crystallization at the melting temperature T_m producing the equilibrium structure characterized by an orientational and translational order. Many molecular crystals form plastic phases at higher temperatures that are stable equilibrium structures which exhibit a dynamical orientational disorder according to the Boltzmann distribution for the reorientational degrees of freedom and a translational order of positions of molecular centers of mass. As temperature decreases they undergo a transition into orientationally ordered equilibrium phase. Some systems show a tendency to form undercooled, metastable liquid states before nucleation and crystallization occur. The range of undercooling depends strongly on molecular properties, but it can be modified significantly by impurities and the effects of temperature or heat flow. It is generally assumed that the presence of impurities and a rapid temperature quench strongly reduces the range of undercooling. The undercooled liquids are metastable structures that may crystallize when they reach experimentally accessible conditions. They may crystallize into a stable equilibrium crystal phase or into an orientationally disordered solid state that is out of equilibrium, and it is called "glassy crystal".[1−4] The final structure depends strongly on quenching rate and the aging temperature, and it is intuitively suggested that a rapid temperature quench, where the enthalpy of freezing can be quickly carried away by the surrounding fluid, leads to glassy crystal structures. The "glassy crystal" is a crystal in the sense that it has translational order and the structure factor S_q determined, e.g., by X-ray scattering looks qualitatively like the one for a crystal, but its orientational degrees of freedom have been frozen at the orientational configuration typical for higher temperatures. A glassy crystal has numerous similarities with conventional glassy state; it exhibits a thermodynamic glass transition characterized by a heat capacity jump, Vogel-Fulcher behavior of the relaxation.[5] Glassy crystals differ from plastic crystals because their orientational disorder represents the state out of equilibrium with respect to the equilibrium orientational distribution exhibited by plastic crystals at a given temperature. There is a broad group of systems that cannot reach experimentally accessible conditions to crystallize. In this case, the normal liquid below the melting temperature T_m changes into the state called a supercooled liquid and finally the system becomes a glassy phase for $T < T_g$, where T_g is called the calorimetric glass transition temperature.[6,7] It is solid in the sense that transverse sound waves can propagate, but it shows no translational and orientational order which is characteristic for a crystal. The system is amorphous in the sense that the structure factor S_q looks like the one for a liquid. Some glasses show orientational order,[8] and they are called orientational glasses.

Many different approaches such as lattice models, bifurcation theory, the renormalization group approaches or computer simulations, and the density functional approach have been employed[5,9] for the study of various phase transitions including crystallization and glass transition. Computer simulations of phase transitions have given a great deal of information about stable and metastable phases. The nucleation on a computer was observed in simulations of a small Lennard-Jones system.[10] The $\alpha \rightarrow \beta$ transition between the stable solid phases of nitrogen[11] or metastable structures of the cyanoadamantane crystal[12] was studied by Monte Carlo method. However, computer simulations also have limitations because of the short time scale of simulations, system sizes, and simplified representation of the intermolecular interaction.

The aim of the present study is to characterize the polymorphism and to identify the phases that are generated in phenylacetylene (PA) in liquid solutions and frozen matrixes. Some PA derivatives are of particular interest with regard to the most recent liquid crystal technologies including polymer-dispersed

* To whom correspondence should be addressed. E-mail: abramczy@mitr.p.lodz.pl.

10.1021/jp011199k CCC: $22.00
Published on Web 01/17/2002

liquid crystals (PDLC) and other confined geometries formed by polymer and porous networks.

To understand the polymorphism of PA derivatives in polymer host matrixes, it seems that the part of this task is finding a suitable simple model system to avoid contribution from too many effects. PA and also mixed compounds with acetonitrile seem to be particularly interesting examples of systems that are suitable for exploration of different stable and metastable phases. In this paper, we hope to understand the competition between the different stable and metastable phases in PA solutions that depend on factors such as interactions with impurities, concentration, temperature, and quenching rate. To understand the structure of the PA solution in liquid and solid phases at a molecular level, we have used vibrational Raman spectra as a physical probe to study them. We will study various structural and dynamical aspects of stable and metastable states generated in these systems. In contrast to liquids and crystals, there is a limited number of experimental data on vibrational dynamics in thermodynamic states strongly deviated from equilibrium like supercooled liquids and glasses or glassy crystals. The dynamics, including vibrational dynamics, of undercooled or supercooled states is of particular interest, because interaction effects are stronger than in the normal liquid state. We will show that Raman spectroscopy in temperature range of 293−10 K provides useful information about the nature of phase transitions at the molecular level and it is a very powerful tool to characterize polymorphism of the system and to identify the stable and metastable phases.

We have recorded the Raman spectra of the ν_s(≡C−H) stretching mode as well as Raman spectra in the lattice region 15−200 cm^{-1} of PA in solutions in the temperature range of 77−293 K as a function of concentration, temperature, and quenching rate.

2. Experiment

Spectrograde acetonitrile and PA were purchased from Aldrich. Acetonitrile was used without further purification. PA was distillated under vacuum before preparing solutions.

The Raman spectra were recorded in the cryostat (Oxford Instruments Limited), and commercial glass ampules were mounted in a special cell arrangement. The samples were introduced as a liquid, and they were cooled in the cryostat equipped with a heater and thermocouples for temperature monitoring. Cooling of the sample was achieved by the use of a 50 L liquid-nitrogen Dewar which supplied a small stream of liquid nitrogen or helium through a vacuum jacketed tube to the cryostat coat. To ensure that the equilibrium phases are generated, the samples were cooled slowly (0.5 °C/min). The differential scanning calorimetry (DSC) method has been used to monitor the phase transitions. The DSC traces were measured during the heating of the frozen samples as well as the cooling of the liquid samples at the rate of 0.5 °C/min at 1 atm pressure with a Netzsch DSC 200 instrument in ampules of 80 mg. The nonequilibrium phases were generated at the rapid temperature quenching in special homemade rings immersed in liquid nitrogen. Liquid solutions of PA were injected into the ring. This procedure ensures the maximum possible quenching rate, in contrast to the slow cooling of 0.5 °C/min used for generation of equilibrium phases. This procedure corresponds to the deposition of an amorphous film or direct sublimation of the sample on the support at 77 K used previously to obtain phases strongly deviated from equilibrium.[13]

Raman spectra were measured with Ramanor U1000 (Jobin Yvon) and Spectra Physics 2017-04S argon ion lasers operating at 514 nm. The spectra corresponding to the Raman lattice region 15−200 cm^{-1} and the ≡C−H modes of PA in acetonitrile were measured. Spectra were recorded in a broad temperature range from 293 to 77 K. The spectral slit width was 1.3 cm^{-1} in the full temperature range, which corresponds to the 200 μm mechanical slit of the spectrometer.

The signal-to-noise ratio in liquid solutions is about 70:1. A similar ratio is observed in frozen matrixes at higher concentrations of PA, whereas at lower concentrations, the ratio is lower, being about 20:1 in the worst cases. The smaller ratios come from the fact that measurements in the cryostat always give lower intensities of the signals than in the standard liquid couvette and that going to lower temperatures the intensity decreases drastically at around 200 K in comparison with the liquid phase.

The interference filter has been used to purify the laser line by removing additional natural emission lines which interfere with the Raman lines, especially in the case of solid samples.

3. Results and Discussion

Figure 1 parts a-c shows a DSC scan of pure PA, PA in acetonitrile, and pure acetonitrile, respectively. The diagram in Figure 1a shows a large melting-like endotherm signal that starts at around 230 K corresponding to the solid phase−liquid transition and a large exotherm signal at 203 K corresponding to the undercooled liquid−solid-phase transition. Figure 1b shows that there are two peaks for PA in acetonitrile both in the endotherm and the exotherm signals. This pattern of behavior illustrates that two separate phases, corresponding to PA and acetonitrile, are formed at lower temperatures. For comparison, Figure 1c shows DSC signals for pure acetonitrile.

Figure 2 shows the Raman band shapes of the stretching mode ν_s(≡C−H) of PA as a function of temperature in acetonitrile. Compared to the results over the equilibrium liquid range, where the band shapes are structureless, the system demonstrates spectacular changes at lower temperatures. The broad, structureless band is transformed into two narrow, temperature-dependent peaks at 3260 and 3271 cm^{-1} at 77 K, and a weak broad band at around 3284 cm^{-1} is also observed.

We first need to ask about the origin of the vibrational substructure of the ν_s(≡C−H) mode observed in Figure 2 for PA in acetonitrile at lower temperatures. The factor group splitting (Davydov splitting) would be appealing as a reason for the splitting as it is typical for crystal solid phases which may occur for PA in acetonitrile at low temperatures. To determine if the factor group splitting leads to the observed changes, we have performed the studies on the band shapes upon concentration dilution and isotopic substitution. If the factor group splitting occurs, the multiplet structure of pure or nonsubstituted crystal should be perturbed severely upon dilution or isotopic substitution because a number Z of the identical molecules in the crystal unit cell is modified.

Figures 3 and 4 show the Raman band shapes of the stretching mode ν_s(≡C−H) as a function of PA concentration in acetonitrile at 77 K for slow and rapid quenching, respectively. We have found that the components at 3260 and 3271 cm^{-1} remain similar in the broad concentration range, whereas at higher concentrations of PA and in pure PA, additional splitting is observed into the components peaked at 3260, 3264, 3266, 3272, 3276, and 3278 cm^{-1}. The results obtained from dilution experiments make clear that the components at 3260 and 3271 cm^{-1} of the ν_s(≡C−H) mode for PA in acetonitrile do not originate from the factor group splitting, but they are further split at higher PA concentrations, each of them into three

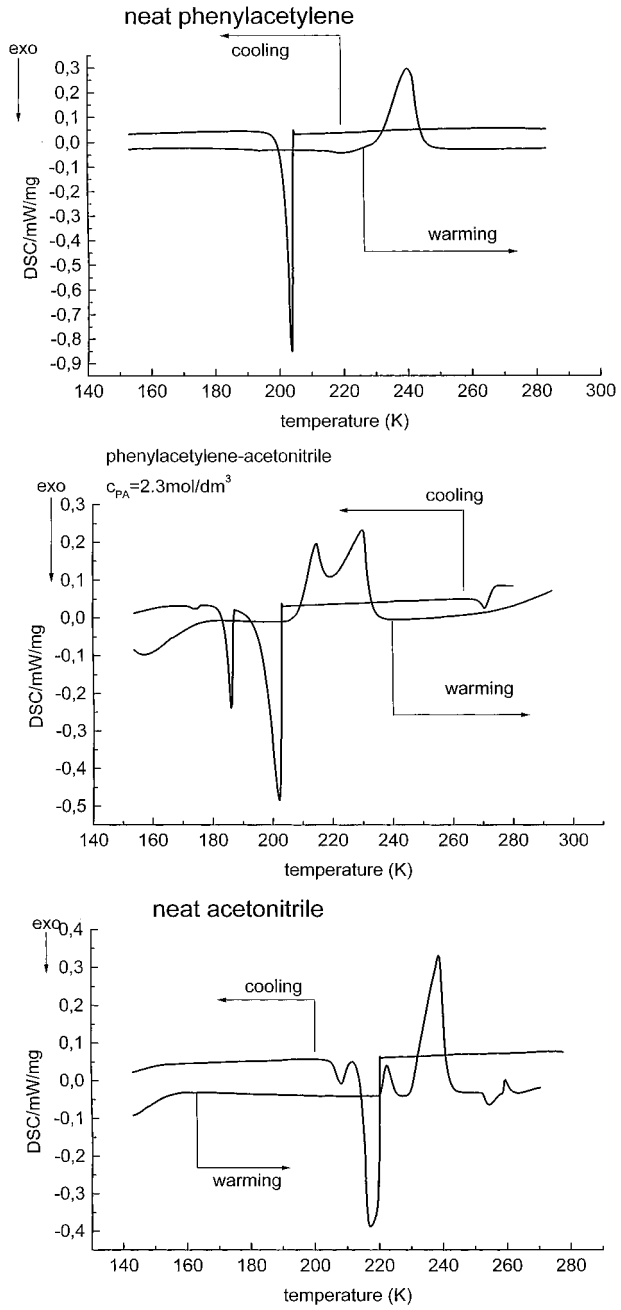

Figure 1. Differential scanning calorimetry (DSC) signals for cooling and warming of the sample: (a) neat phenylacetylene, (b) phenylacetylene in acetonitrile (c = 2.3 mol/dm^3), and (c) neat acetonitrile.

components, because of this effect. It means that the peaks at 3260 and 3271 cm^{-1} must illustrate the coexistence of two solid phases, each of them of the crystalline origin, because the factor group splitting may occur in only crystals.

To learn more about the origin of the vibrational substructure of the bands for PA, it would be valuable to comment on the influence of a quenching rate on the generated phases. It is generally assumed that rapid cooling leads to glass formation, whereas slow cooling results in crystallization.[1−5] Comparing the results obtained for the slow cooling in Figure 3 and those for the rapid quench in Figure 4 we can state that the Raman spectral features are nearly identical for PA in acetonitrile solutions: two narrow peaks at 3260 and 3271 cm^{-1} and a weak broad band at 3284 cm^{-1}. These results provide a strong indication that in both cases the similar phases are generated: two crystalline phases and a small fraction of a disordered phase

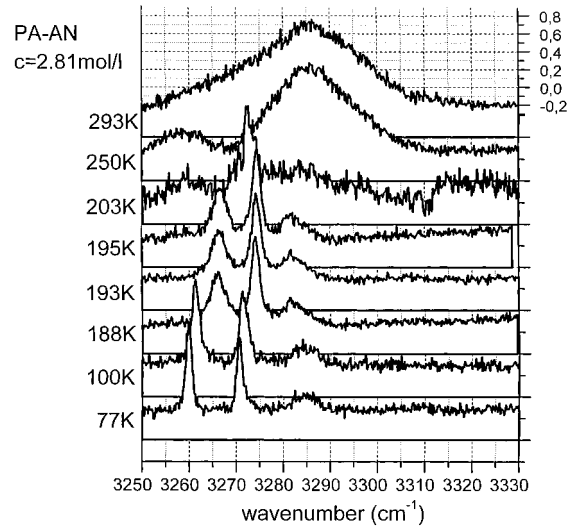

Figure 2. Raman spectra of the ν_s(≡C−H) mode of phenylacetylene in acetonitrile (c = 2.81 mol/dm^3) as a function of temperature (slow cooling).

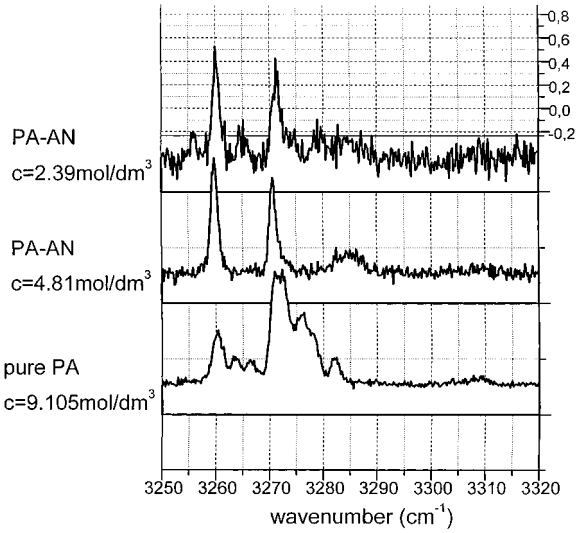

Figure 3. Raman spectra of the ν_s(≡C−H) mode of phenylacetylene in acetonitrile as a function of concentration at 77 K (slow cooling).

represented by a broad band at 3284 cm^{-1}. In both cases, we observe the factor group splitting of the components at 3260 and 3271 cm^{-1} at higher PA concentration, but the rapid quench leads to more a pronounced effect indicating a more prominent signature of the crystalline phases. Moreover, for the rapid quench in Figure 4 the frequencies of the components at 3256, 3260, 3265, 3272, 3276, and 3278 cm^{-1} are slightly different from those observed in Figure 3 for the slow cooling which may suggest different topologies of the phases generated during the slow and rapid quench.

Figure 5 shows the effect of the deuterium substitution in PA−PA-d_6 mixtures on the ν_s(≡C−H) stretching mode of PA for the rapid quench. The deuteration results in the isotopic mixtures of PA and deuterated PA-d_6 show exactly the same picture: two components at 3260 and 3271 cm^{-1} in the substitution range from the mole fraction of nondeuterated PA x_{PA} = 0.0−0.75 and the further splitting of each component for higher PA concentrations up to pure PA at x_{PA} = 1.0. These results make once again abundantly clear that the components at 3260 and 3271 cm^{-1} are not the results of the factor group splitting but each component is further split because of this effect

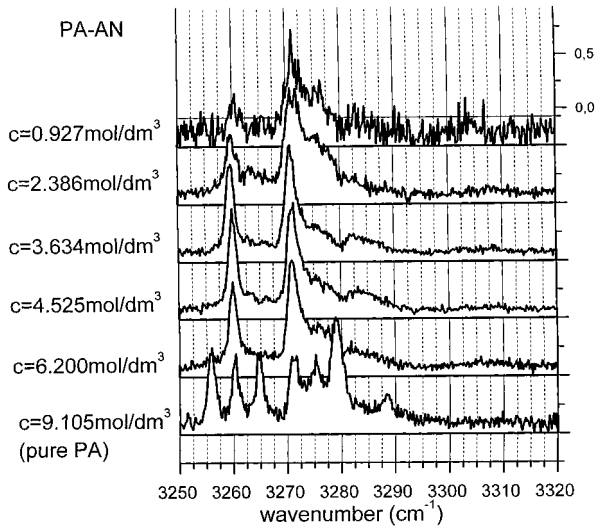

Figure 4. Raman spectra of the ν_s(≡C—H) mode of phenylacetylene in acetonitrile as a function of concentration at 77 K (rapid quenching).

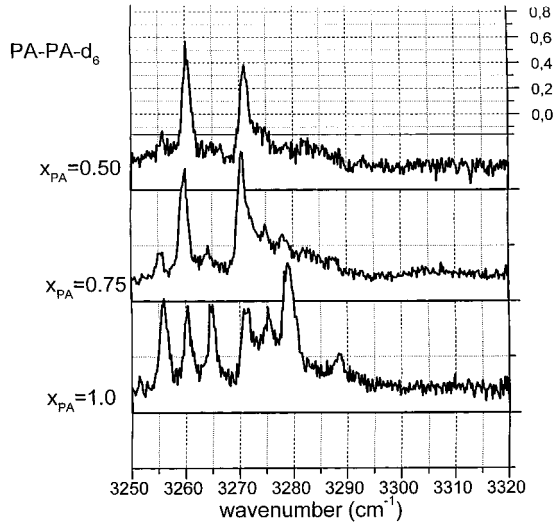

Figure 5. Raman spectra of the ν_s(≡C—H) mode of phenylacetylene in a mixture of PA and deuterated PA as a function of isotopic substitution for $x_{PA} = 1.0$, 0.75, and 0.5, where x_{PA} is a mole fraction of phenylacetylene.

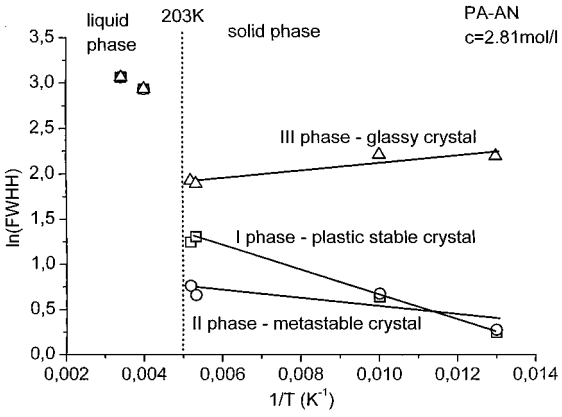

Figure 6. Logarithm of the Raman bandwidth (fwhh) of the ν_s(≡C—H) mode of PA in acetonitrile ($c = 2.81$ mol/dm^3) for the components at 3260 (□), 3272 (○), and 3285 cm^{-1} (△) as a function of temperature.

at higher PA concentration. The site group splitting can be ruled out because the ν_s(≡C—H) mode has A_1 symmetry.

The picture that emerges from the analysis of the results in Figures 2−5 is as follows. The highest frequency broad band

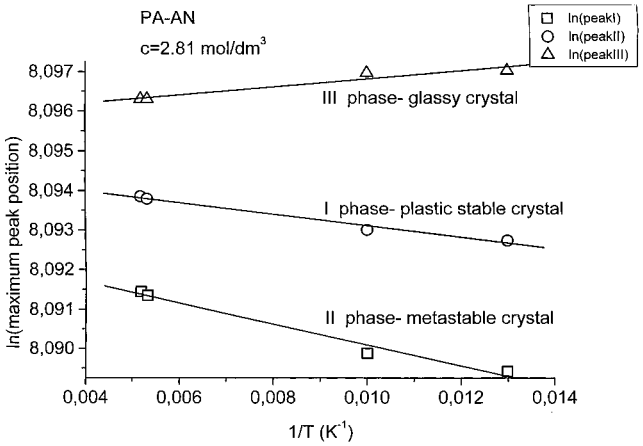

Figure 7. Logarithm of the Raman maximum peak position of the ν_s(≡C—H) mode of PA in acetonitrile ($c = 2.81$ mol/dm^3) for the components at 3260 (□), 3272 (○), and 3285 cm^{-1} (△) as a function of temperature.

at 3284 cm^{-1} represents a strongly disordered phase, whereas the two narrow peaks at around 3260 and 3271 cm^{-1} represent crystalline phases, with one of them supposed to represent the metastable configuration with respect to the equilibrium crystal structure. The question arises what the differences between these two crystal phases are. Establishing the symmetries of the components corresponding to these phases from Raman measurements in the polarized light would be very helpful, but the polycrystalline nature of the sample does not allow us to do this.

So far, we were mainly concentrated on the static vibrational properties of the phases generated in PA represented by the maximum peak positions. However, it is important to remember that the Raman band shapes and the bandwidths are a very important probe in rationalizing dynamics of molecular processes occurring in different phases.[16] Even more informative than knowing the magnitude of Raman band broadening at phase transitions is the Arrhenius plot of the line width versus temperature which may tell us which kinds of motions of solvent molecules are most efficient in dissipating vibrational energy or vibrational dephasing. The Arrhenius plot may help us to estimate the activation energy ΔE of the vibrational relaxation mechanism. When an Arrhenius plot is linear, it indicates that only a single low energy mode is involved in the temperature dependence of the relaxation process, and the slope of the plot gives the frequency of the mode coupled to the relaxing vibrational mode.

Figure 6 shows the Arrhenius plot for the stretching mode ν_s(≡C—H) of PA in acetonitrile as a function of temperature. We can see that the bandwidth of the broad structureless band observed in the liquid phase shows the dramatic change at around 203 K, and this band is split into three components at around 3260, 3271, and 3284 cm^{-1}.

Figure 7 shows the Arrhenius plot for the maximum peak positions of the components as a function of temperature. One can see that both the bandwidth and the maximum peak position of the components assigned to the crystal phases at 3260 and 3271 cm^{-1} decrease, whereas those of the component at 3284 cm^{-1} assigned to the glassy crystal phase increases with temperature decreasing. As we can see, the linear plot does fit quite well the experimental data. The experimental data for the components representing the crystal phases at 3260 and 3271 cm^{-1} yield thermal activation energies of 92 ± 4 and 33 ± 13 cm^{-1}, respectively.

The magnitudes of the activation energies cover the range of translational and vibrational optical phonons presented in Figure

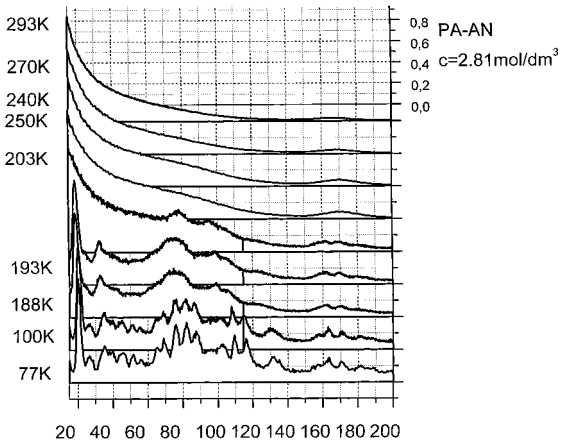

Figure 8. Raman spectra of the lattice region 15−200 cm^{-1} for phenylacetylene in acetonitrile (c = 2.81 mol/dm^3) as a function of temperature.

8. The vibrational component at 3260 cm^{-1} represents the vibrational oscillator coupled to the motions at around 92 cm^{-1} that represent an evidently plastic crystal structure with rotational disorder at the temperatures between 203 and 188 K. Indeed, both the ν_s(≡C−H) component at 3260 cm^{-1} (Figure 2) and the bands around 92 cm^{-1} (Figure 8) are broad in this temperature range, and it is a clear indication of a plastic crystal structure with rotational disorder. Upon temperature decreasing, this structure evolves into the state where orientations of molecules become ordered and the plasticity disappears. Thus, we can state that the component at 3260 cm^{-1} represents the equilibrium stable crystal phase of PA that exhibits plasticity at higher temperatures. The vibrational component of PA in acetonitrile at 3271 cm^{-1} represents the oscillator coupled to the lattice vibrations around 33 cm^{-1} and its bandwidth is much less sensitive to temperature than that of the component at 3260 cm^{-1}. The activation energy of 33 ± 13 cm^{-1} covers the range of the frequency at 20 cm^{-1} in Figure 8, where the very intensive narrow peak is observed. Its temperature dependence yields a thermal activation energy of 24 ± 13 cm^{-1} that is strikingly similar to that obtained for the 3271 cm^{-1} component. In view of these results, it is evident that the vibrational component of the ν_s(≡C−H) mode at 3271 cm^{-1} for PA in acetonitrile represents the same crystal phase as the component at 20 cm^{-1}in the Raman lattice spectrum. Taking into account that the band broadening mechanisms of the profiles representing this phase are weakly thermally activated, we can state that this crystal phase shows no signatures of plasticity and it comes from the metastable structure relative to the stable crystal structure represented by the 3260 cm^{-1}.

4. Conclusions

A parallel use of DSC and Raman spectroscopy in the temperature range of 293−77 K has allowed us to reveal and characterize the low temperature polymorphism of the mixtures of PA in acetonitrile in the full concentration range. We have found that the low temperature polymorphism of PA strongly depends on the temperature, concentration, and quenching rate. The essential finding are as follows:

(i) There exist two equilibrium crystal phases for PA in acetonitrile for the concentration range $0 < c < 6.2$ mol/dm^3 with a small contribution from a glassy crystal or glassy phase. The polymorphism of PA in acetonitrile is similar for the rapid and slow cooling.

(ii) The crystal phase represented by the peak at 3260 cm^{-1} forms plastic, or so-called rotator, phase below the liquid−solid transition for the temperatures between 203 and 100 K. Upon temperature decreasing, they evolve into the state where also orientations of molecules become ordered (crystal phase I)

(iii) The second crystal phase (represented by the peak at 3271 cm^{-1}) is metastable with the respect to crystal I. In contrast to phase I, the metastable crystal phase (crystal II) exhibits no signatures of plasticity at higher temperatures.

(iv) Vibrational relaxation processes occurring in the stable and metastable phases are thermally activated by single low energy modes. The ν_s(≡C−H) oscillator of the stable crystal phase I is coupled to the mode of the frequency at 92 cm^{-1}, whereas that of the metastable crystal phase II is coupled to the lattice mode at 20 cm^{-1}.

References and Notes

(1) Delcourt, O.; Descamps, M.; Even, J.; Bertault, M.; Willart, J. F. *Chem. Phys*. **1997**, *215*, 51−57.

(2) Kuchta, B.; Rohleder, K.; Etters, R. D.; Belak, J. *J. Chem. Phys*. **1995**, *102*, 3349.

(3) Willart, J. F.; Descamps, M.; Benzakour, N. *J. Chem. Phys*. **1996,** *104*, 2508.

(4) Kuchta, B. *J. Chem. Phys*. **1998,** *109*, 6753.

(5) Götze, W. In *Liquids, freezing and glass transition*; Hansen, J. P., Levesque, D., Zinn-Justin, J., Eds.; North-Holland: Amsterdam, The Netherlands, 1991; p 289.

(6) Alba-Simionesco, C.; Fan, J.; Angell, C. A. *J. Chem. Phys*. **1998**, *110*, 5262.

(7) Ferrer, M. L.; Lawrence, Ch.; Demirjian, B. G.; Kivelson, D. *J. Chem. Phys*. **1998**, *109*, 8010.

(8) Michel, K. H. *Z. Phys. B: Condens. Matter* **1987** *68*, 259.

(9) Oxtoby, D. In *Liquids, freezing and glass transition*; Hansen, J. P., Levesque, D., Zinn-Justin, J., Eds.; North-Holland: Amsterdam, The Netherlands, 1991; p 145.

(10) Mandell, M. J.; Mclaque, J. P.; Rahman, A. *J. Chem. Phys*. **1976**, *64*, 3699.

(11) See ref 2.

(12) Kuchta, B.; Descamps, M.; Affouard, F. *J. Chem. Phys*. **1998**, *16*, 6753.

(13) Johari, G. P.; Hallbrucker, A.; Mayer, E. *J. Chem. Phys.* 1**990**, *92*, 6743.

(14) Pinan, J. P.; Quillon, R.; Ranson, P.; Becucci, M.; Califano, S. *J. Chem. Phys*. **1998**, *109*, 5469.

(15) Brozek, B.; Abramczyk, H. *Chem. Phys*. **1999**, *250*, 35.

(16) Madden, P. A. In *Spectroscopy and Relaxation of Molecular Liquids*; Steele, D., Yarwood, J., Eds.; Elsevier: Amsterdam, The Netherlands, 1991.

(17) Oxtoby, D. W. *Adv. Chem. Phys*. **1979**, *40*, 1. Oxtoby, D. W. *Adv. Chem. Phys*. **1981**, *41*, 487.